ITCsF2 TAI EVALUATION
MJD 57199-57229 (26/6/2015-25/7/2015)

Introduction

During the period MJD 57199-57229 INRIM has evaluated the frequency of its Hydrogen Maser IT-HM3 (BIPM code 1401103) using the Cs fountain primary frequency standard ITCsF2. The evaluation procedure of the fountain standard follows the general procedures reported in [1]; we report here details on the Type A and Type B uncertainty evaluation, together with the internal transfer uncertainty (including the contribution of dead time).

ITCsF2 Accuracy Evaluation

Black Body Radiation Shift $\Delta\nu_{BBR}$

The evaluation of the Blackbody Radiation (BBR) Shift $\Delta\nu_{BBR}$ requires to know the effective BBR temperature T experienced by the atoms along their ballistic flight. For the calculation of T, we use the temperature data coming from three RTD positioned along the drift tube. Given the low temperature of the interaction region resulting from cryogenic cooling the maximum temperature gradient is conservatively taken also to estimate the uncertainty of the correction. We use the well known relation

$$\frac{\delta\nu_{BBR}}{\nu_{Cs}} = \beta\left(\frac{\Theta}{300}\right)^4\left[1+\varepsilon\left(\frac{\Theta}{300}\right)^2\right] \qquad (1)$$

where Θ is the blackbody temperature, β=-1.718(3)×10^{-14} and ε=1.3(1)×10^{-2} [2-3]. As the thermodynamic temperature of ITCsF2 drift region is Θ=(89.4 ± 2.0) K, the blackbody radiation shift is $(-1.36\pm0.09)\times10^{-16}$. Taking into account the small solid angle aperture to the external environment at room temperature (296 K), the final correction is:

$$\frac{\delta\nu_{BBR}}{\nu_{Cs}} = \left(-1.45\pm0.12\right)\times10^{-16}.$$

Gravitational Red Shift $\Delta\nu_{RS}$

Gravitational redshift at the ITCsF2 location was accurately calculated during 2006 (details in [4]) and the result from that activity is used here to correct the TAI calibration data. The orthometric height (above the Geoid) of ITCsF2 has been evaluated using refined gravimetric data, coming from an accurate Geoid regional model (ITALGEO99) and levelling. The orthometric height of ITCsF2 is h = (238.7±0.1) m, leading to a gravitational redshift $\Delta\nu_{RS}$:

$$\frac{\delta\nu_G}{\nu_{Cs}} = (260.4\pm0.1)\times10^{-16}$$

Quadratic Zeeman Shift $\Delta\nu_Z$

The effective C-field experienced by the atoms (B_0) along their trajectory is calculated (see [1] for details) from a field map which is obtained measuring the low frequency magnetic resonance transitions when the atoms are at the apogee; the map is completed launching the atoms at different apogee heights. The map is used to estimate the position of the central fringe of the Ramsey spectroscopy of the magnetic sensitive transition $|$F=4, m_F=1$> \rightarrow |$F=3, m_F=1$>$. Its frequency is compared to the frequency of the Majorana transition $|$F=3, m_F=0$> \rightarrow |$F=3, m_F=±1$>$, that is used to monitor the magnetic field value along the whole TAI measurement.

The Majorana resonance transition is not a good representation of the magnetic field along the Ramsey flight, because the amplitude of the applied field can change from place to place and its penetration depth in the interaction region is not constant (because of different wall thickness).

Consequently, a wrong weight of the local field along the atom free flight is expected. Nonetheless, for small fluctuations of the magnetic field, an excellent linearity was observed between the magnetic field value measured with the Ramsey spectroscopy and the Majorana measurement; once calibrated, this allows to precisely track the field variations.

Since the magnetic sensitive transition is used to determine the Zeeman shift, an additional contribution to the bias uncertainty is the difference Δ_B between the time average of the squared magnetic field B and the square of the time averaged field:

$$\Delta_B = \frac{1}{T}\int_0^T B^2\,dt - \left(\frac{1}{T}\int_0^T B\,dt\right)^2$$

From the analysis of the recorded C-field map, the difference is $\Delta_B \leq 6.5\times10^{-18}$ T^2; using the sensitivity coefficient of the second order Zeeman shift (427.45×10^8 Hz/T^2), the contribution to the bias uncertainty is $\leq 3\times10^{-17}$. Combining all the contributions, the total uncertainty for the magnetic field correction is 0.8×10^{-16}. Therefore, the average second order Zeeman bias $\delta\nu_Z$ relative to the clock frequency ν_{Cs} is

$$\frac{\delta\nu_Z}{\nu_{Cs}} = (1081.6\pm0.8)\times10^{-16}$$

The daily value of the shift on the clock transition is reported in Figure 1.
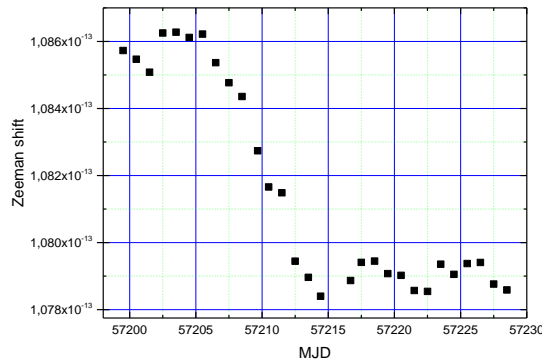

Figure 1. Zeeman shift fluctuations during the TAI evaluation period.

Collisional Shift

The collisional shift is corrected measuring the collisional coefficient. This latter is evaluated alternating operation at two different densities, labelled HD (high density) and LD (low density). The average density ratio between HD and LD conditions is about 3 and the total accumulated run time at LD is 1.5 times larger than in HD, as in LD the stability is degraded by the low atom number.

This technique assumes that the proportionality between the density and the atomic signal (the parameter which is actually detected) is constant during the whole run. This proportionality is confirmed by the recorded TOF signal analysis taken in HD and LD both on the way up and on the way down.

During the present evaluation we used a constant loading time of 400ms along the whole evaluation period, using collisional coefficient derived from previous evaluations.

We measured an average value of the density shift and an associated type B uncertainty of:

$$\frac{\delta v_{coll}}{v_{Cs}} = (-8.0 \pm 2.3) \times 10^{-16}$$

Microwave related Shifts

As reported in [1] the microwave related shifts (e.g. microwave leakage, DCP, spurs in the spectrum, lensing effect, 2nd order cavity pulling) were carefully evaluated in ITCsF2.
The performed tests involved frequency measurements at different excitation power ($\pi/2$, $3\pi/2$ and $5\pi/2$), as well as frequency measurements tilting the fountain on the East-West and North-South axes. Also, measurements were performed with symmetric and asymmetric feeding, in order to better characterize the various shifts.
There is no evidence of DCP shift at the level of 2×10^{-17}, and of 2nd order cavity pulling at 3×10^{-17}, whilst the microwave leakage $\delta v_{\mu W}$ shift is corrected for:

$$\frac{\delta v_{\mu W}}{v_{Cs}} = (-1.2 \pm 1.4) \times 10^{-16}$$

Since these tests are complicate and require several months of measurement, until modifications are not implemented on ITCsF2, we will use the shift and the related uncertainty reported in [1].

Summary of accuracy evaluation (type B)

Physical effect	Bias (10^{-16})	Uncert. (10^{-16})
Zeeman effect	1081.6	0.8
Blackbody radiation	-1.45	0.12
Gravitational redshift	260.4	0.1
Microwave leakage	-1.2	1.4
DCP	-	0.2
2nd order cavity pulling	-	0.3
Background gas	-	0.5
Atomic density	-8.3	2.4
Total Type B	**1331.1**	**3.0**

Table 1. Summary of corrected and uncorrected shifts and uncertainty budget for ITCsF2, during the reported period.

Evaluation of the average frequency y(ITCsF2) - y(HM3)

During the reported evaluation period, the H-maser HM3 (BIPM code 1401103) was used as local oscillator.

The average frequency *y(ITCsF2) - y(HM3)* over that period was calculated with a classical linear fit. First, the row data are density shift corrected and then they are fitted using a linear equation of the following form:

$$y = a + ct$$

which fits the data *(yᵢ, tᵢ)* where the y_i is the value of the measurement *y(ITCsF2) - y(HM3)* taken at the epoch t_i The meaning of the parameter *a*, which can be regarded as *y(t=0)*, is the estimation of the average frequency *y(ITCsF2) - y(HM3)* extrapolated to zero density if the epoch coordinate origin is taken on the centre of the evaluation interval (MJD 57184). The parameter *c* is the average maser drift over the evaluation period.

Fitting the maser drift over the evaluation epoch was chosen because fountain dead (lost) time is unavoidable during the evaluation period, and the dead time intervals are neither evenly spaced nor symmetric with respect to the centre of the evaluation period. In these conditions, dead time would have biased an estimation derived by a standard average. Epoch distribution of fountain dead time is reported in Figure 2.
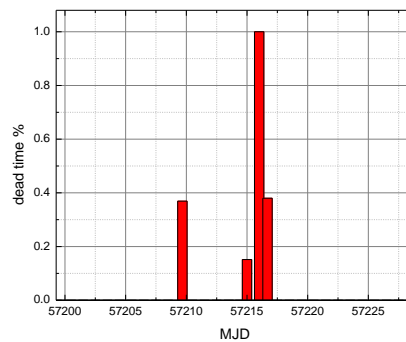

Figure 2. Epoch distribution of the dead time during the present evaluation.

The choice of a linear model for the maser drift takes into account the fact that the HM3 frequency has shown a very stable drift in the past year within periods even longer than 50 days.

The uncertainty associated to the average frequency estimation *y(ITCsF2) - y(HM3)* and reported as Type A, is the uncertainty of the coefficient a as it is estimated by the least square algorithm. Figure 3 shows *y(ITCsF2) - y(HM3)* data (extrapolated to zero density).
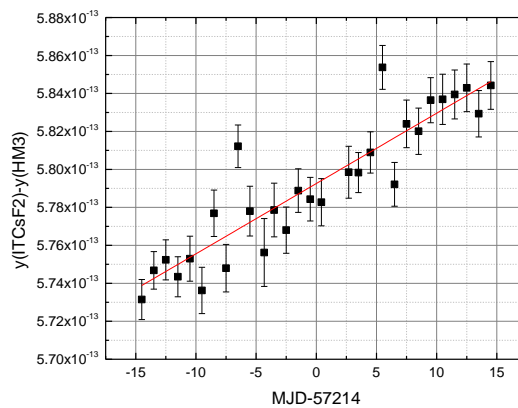

Figure 3. *y(ITCsF2) - y(HM3)*- data and the linear fit curve (straight line).

Final results of the statistical analysis are reported in Table 2:

	Value	Uncertainty
HM3 drift (*Coefficient c*)	3.7×10^{-16} /day	0.3×10^{-16} /day
y(ITCsF2) - *y(HM3)* extrapolated to zero density, MJD 57214 (*Coefficient a*)	$+579.26 \times 10^{-15}$	0.29×10^{-15}

Table 2. Results of the statistical analysis.

Local link and dead time uncertainty (ul/lab)

The HM3 is phase compared to the UTC(IT) time scale, which is the reference time scale for remote time and frequency transfer tools, with a Time Interval Counter in the INRIM Time and Frequency laboratory. This comparison introduces an uncertainty contribution to the ITCsF2 transfer to TAI, which is estimated as 0.1×10^{-15} for this evaluation period (30 days).

The dead time in fountain operation introduces a further uncertainty to the frequency transfer to TAI. The estimation of this uncertainty contribution requires the knowledge of the HM3 noise properties.
The stability of HM3 could be modelled in terms of Allan variance, as:

$$\sigma_y^2(\tau) = \sigma_{yWF}^2(\tau) + \sigma_{yFF}^2(\tau) + \sigma_{yRW}^2(\tau)$$

where $\sigma_{yWF}^2(\tau)$, $\sigma_{yFF}^2(\tau)$ and $\sigma_{yRWF}^2(\tau)$ are respectively the contribution due to white, flicker and random walk frequency noise. A conservative estimation of these contributions is:

$$\sigma_{yWF}(\tau) < 3 \cdot 10^{-13} \tau^{-1/2}$$

$$\sigma_{yFF}(\tau) < 3 \cdot 10^{-16}$$

$$\sigma_{yRW}(\tau) < 2 \cdot 10^{-19} \tau^{1/2}$$

The dead time uncertainty contribution is calculated from the theory reported in [5], and from a software routine [6], that implements a refined algorithm with respect to [5]. This method can handle the actual dead time distribution of the fountain run and provides an estimation of the dead time uncertainty. The dead time uncertainty contribution, calculated for the distribution shown in Fig 2 using the software routine [6] is reported in the table below.

Contribution	Uncertainty (10^{-15})
HM link to UTC(IT)	0.1
Fountain Dead Time (6%)	0.06
Total (ul/lab)	**0.12**

Table 3. Contributions to ul/lab.

Summary of TAI evaluation results.

The final evaluation is obtained using the data reported in Table 2

MJD Period	y(HM3- ITCsF2)	uA	uB	ul/lab	uRef
57199-57229	-579.26 $\times 10^{-15}$ (*)	0.29×10^{-15}	0.30×10^{-15}	0.12×10^{-15}	[1]

Table 4. Final results of ITCsF2 evaluation.

(*) HM3 has the BIPM code 1401103

References

[1] F. Levi et al. Accuracy evaluation of ITCsF2: a Nitrogen cooled Cesium Fountain,(2014), Metrologia vol. 51 n. 3, 270-284

[2] E. Simon et al., (1998) Phys. Rev A 57, 436

[3] E.J. Angstmann, V.A., Dzuba V. Flanbaum, (2006) *Phys. Rev. Lett,* 97 040801

[4] D. Calonico, A. Cina, I. H. Bendea, F. Levi, L. Lorini, and A. Godone "Gravitational red-shift at INRIM, Italy". Metrologia 44, L44-L48, (2007).

[5] Y. Dai-Hyuk, M. Weiss and T. E. Parker, "Uncertainty of a frequency comparison with distributed dead time and measurement interval offset" Metrologia 44, 91-96 (2007)

[6] G. Panfilo, T. Parker, Proc. 2007 Joint Mtg. IEEE Intl. Freq. Cont. Symp. and EFTF Conf., 805-810, 2007

[7] T. Parker, G. Panfilo, Proc. 2007 Joint Mtg. IEEE Intl. Freq. Cont. Symp. and EFTF Conf., 986-991, 2007